Electronic Supplementary Information (ESI)

Space-Confined Indicator Displacement Assay inside a Metal-Organic Framework for Fluorescence Turn-On Sensing

*Ning-Ning Yang, Li-Jiao Zhou, Peng Li, Qi Sui, En-Qing Gao**

Shanghai Key Laboratory of Green Chemistry and Chemical Processes, School of Chemistry and Molecular Engineering, East China Normal University, Shanghai 200062 (P. R. China).

*Email: eqgao@chem.ecnu.edu.cn

Physical methods.

^{1}H NMR spectra were recorded on a Bruker Advance 400 MHz spectrometer. The FT-IR spectra were recorded in the range 500-4000 cm^{-1} using KBr pellets on a Nicolet NEXUS 670 spectrophotometer. Powder X-ray diffraction (PXRD) at ambient pressure was recorded on a Rigaku D/Max-2500 diffractometer at 35kV, 25mA for a Cu-target tube and a graphite monochromator. UV-vis diffuse reflectance spectra were measured using a SHIMADZU UV-2700 spectrophotometer, with $BaSO_4$ plates as references (100% reflection). Fluorescence spectra were recorded on a Hitachi F-4500 spectrofluorometer. Nitrogen adsorption and desorption isotherm measurements were performed on a Micromeritics ASAP2020 analyzer at 77K. Thermogravimetric analysis (TGA) experiments were performed on a NETZSCH STA 449 F3.

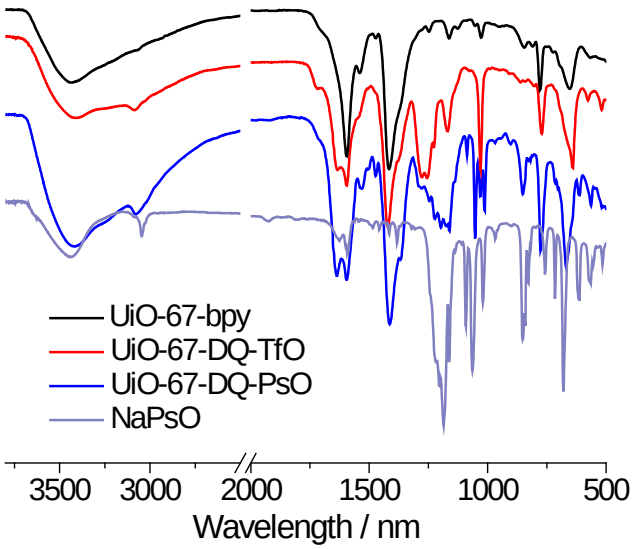

Fig. S1. IR spectra of the NaPsO, UiO-67-bpy, UiO-67-DQ-TfO, and UiO-67-DQ-PsO.

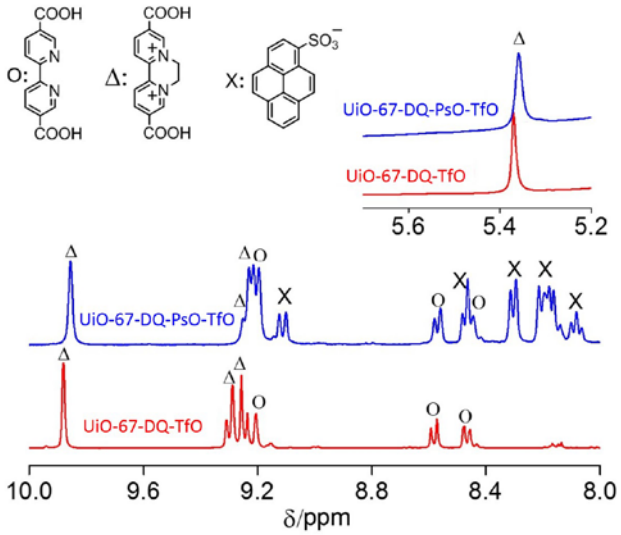

Fig. S2. ^{1}H NMR spectra of the solutions obtained by digesting UiO-67-DQ-TfO (red, N-alkylation ratio: 65%) and UiO-67-DQ-PsO-TfO (blue, N-alkylation ratio: 65%, anion exchange ratio: 67%) with HF (aq.)/d6-DMSO (1/40, v/v). The dashed lines stress the shifts of some peaks.

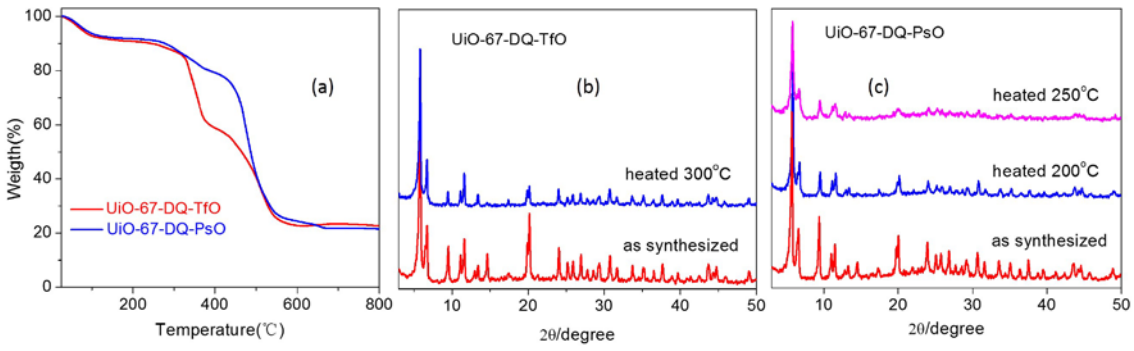

Fig. S3. (a) TGA of UiO-67-DQ-TfO and UiO-67-DQ-PsO. PXRD profiles for UiO-67-DQ-TfO (b) and UiO-67-DQ-PsO (c) before and after heated.

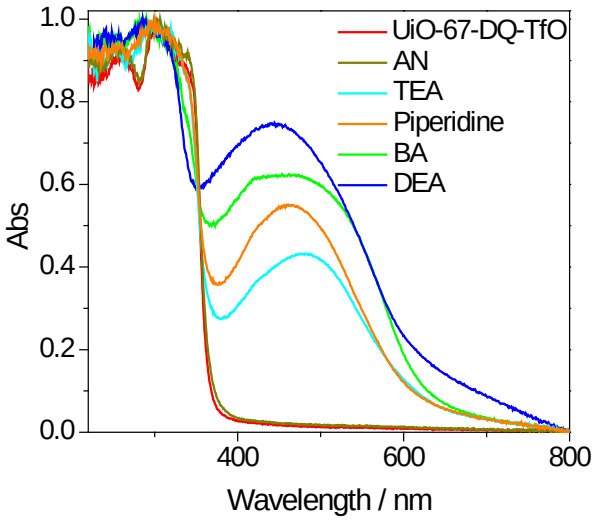

Fig. S4. UV/vis spectra of UiO-67-DQ-TfO before and after exposed to various amines.

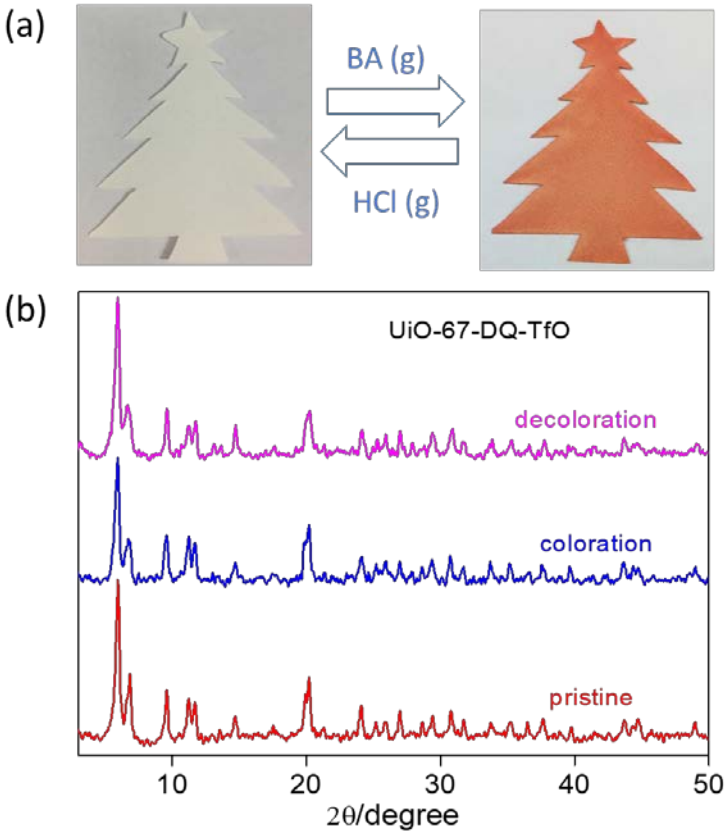

Fig. S5. (a) Color changes of a UiO-67-DQ-TfO-loaded papercut and (b) PXRD patterns of a UiO-67-DQ-TfO sample befor and after coloration with butylamine vapor and after decoloration with hydrogen chloride.

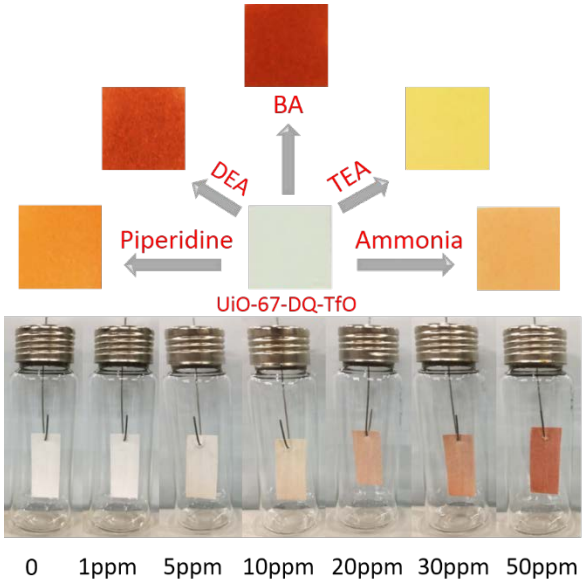

Fig. S6. Naked-eye detection of amines using UiO-67-DQ-TfO-coated test paper. Above: the color change of the test paper upon fuming with different amines. BA = butylamine, DEA = diethylamine, TEA = triethylamine. Below: the color change at different concentrations of BA. And the test papers response to different concentrations of butylamine.

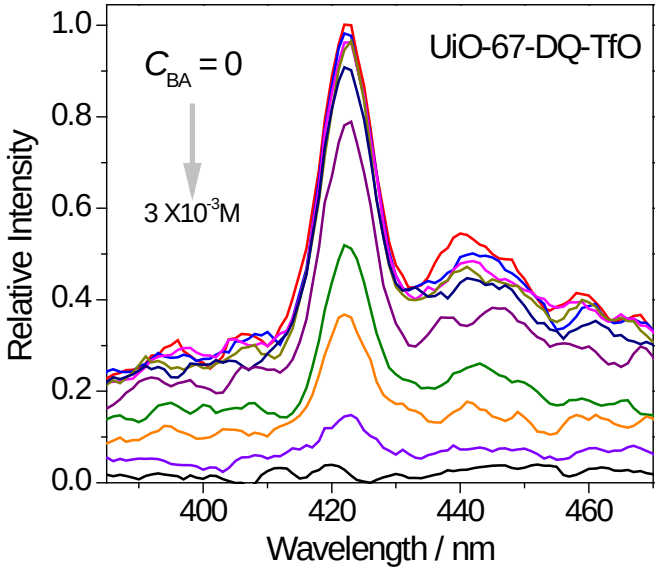

Fig. S7. Fluorescence spectra of the UiO-67-DQ-TfO dispersion in response to butylamine in aqueous solution .

Fig. S8. Colors of NaPsO, UiO-67-DQ-TfO and UiO-67-DQ-PsO before and after exposure to butylamine (BA) vapor.

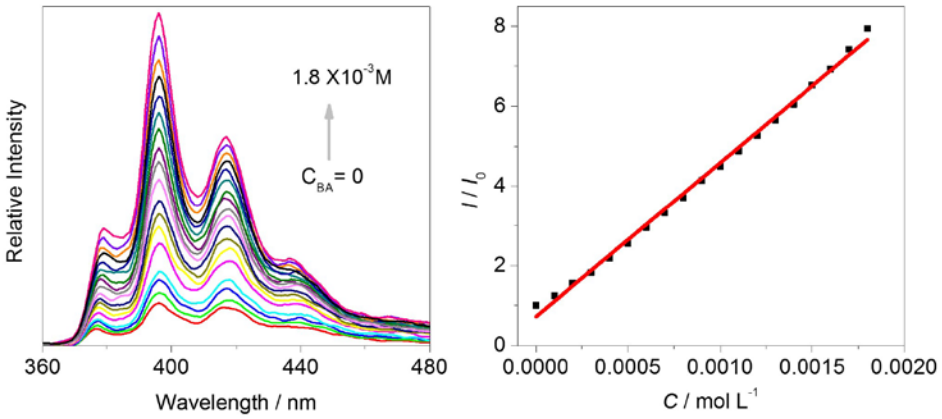

Fig. S9. Variation of fluorescence spectra (left) and I/I_0 (right, 395 nm) of UiO-67-DQ-PsO-TfO upon incremental addition of butylamine.

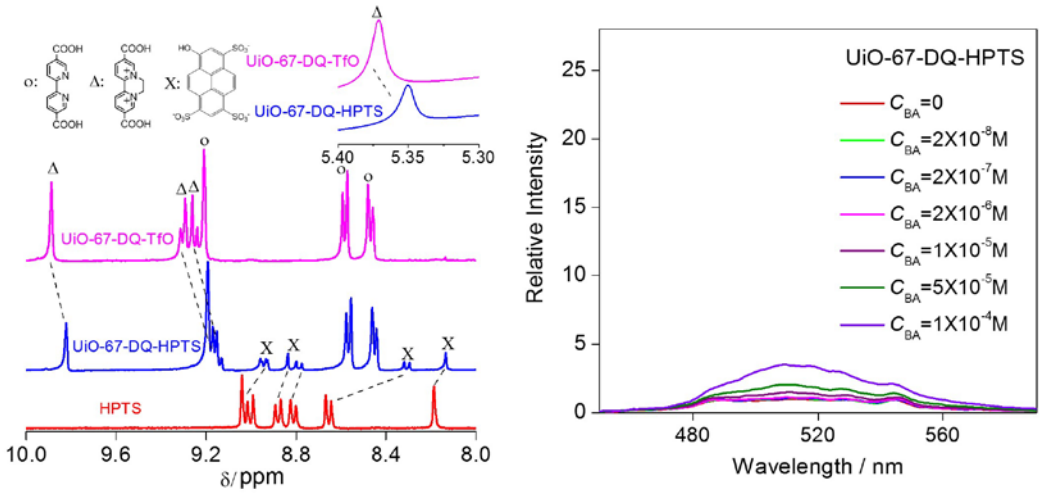

Fig. S10. (Left) ^{1}H NMR spectra of the solutions obtained by digesting Na_3HPTS(red), UiO-67-DQ-HPTS(blue), UiO-67-DQ-TfO (pink) with HF (aq.)/d6-DMSO (1/40, v/v). The dashed lines stress the shifts of some peaks. (Right) Fluorescence spectra of UiO-67-DQ-HPTS solutions upon incremenal addition of butylamine (BA).

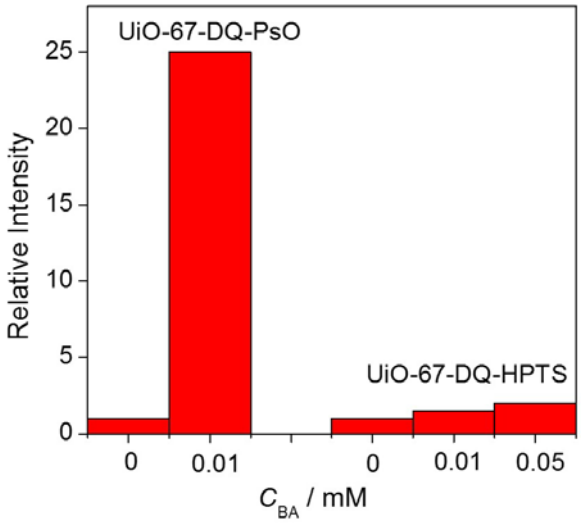

Fig. S11. The fluorescence relative intensity of UiO-67-DQ-PsO (395nm) and UiO-67-DQ-HPTS (510nm) upon before and after added a certain concentration of butylamine (BA).

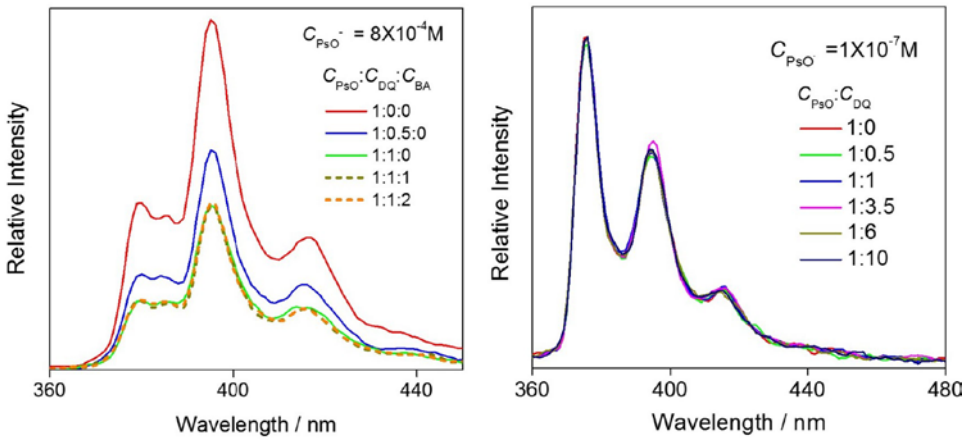

Fig. S12. Fluorescence spectra of NaPsO solutions upon incremenal addition of $DQ(TfO)_2$ and butylamine (BA). Left: The amount of PsO^- is equivalent to that for the UiO-67-DQ-PsO suspension used for sensing experiments. Right: the results obtained at a much lower C_{PsO}, showing that the emission of PsO^- in dilute solution is hardly influenced by DQ^{2+}.

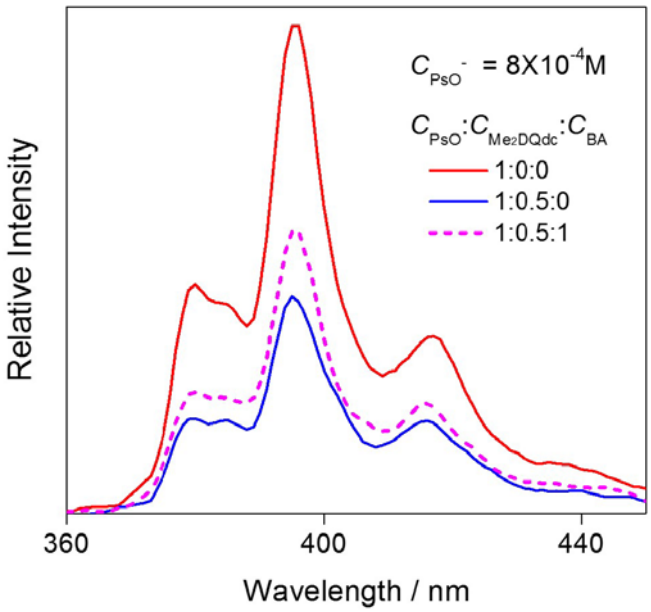

Fig. S13. Fluorescence spectra of NaPsO solutions monitored upon addition of $[Me_2DQdc](TfO)_2$ and butylamine (BA).

Table S1

Comparison of different materials for colorimetric detection of alkylamine vapors.

Materials [a]	Analytes	Detection limit(ppm)	Ref.
MAF	dimethylamine	0.4	1
UiO-68-osdm	diethylamine	10	2
ZZ-HPB-CN	triethylamine	10	3
MS	triethylamine	11.7	4
1b-GFP	propylamine	29	5
UiO-67-DQ-TfO	butylamine	5	This work

[a] MAF = Meldrum's activated furan, MS = a pyrylium-functionalized polymeric membrane, ZZ-HPB-CN = hexaphenyl-1,3-butadiene derivative, 2,2'-((((1Z,3Z)-1,2,3,4-tetraphenylbuta-1,3-diene-1,4-diyl)bis(4,1-phenylene))bis(methanylylidene)) dimalononitrile, 1b-GFP = glass filter paper loaded with a ylidenemalononitile enamine.

Table S2

Comparison of different materials for the determination of DA.

Detection mode	Materials	Detection limit(μM)	Ref.
Fluorescence (Turn-off)	$[UO_2(L)]$	126	6
Fluorescence (Turn-off)	Fe-MIL-88–NH_2	30	7
Fluorescence (Turn-on)	Fe-MIL-88–H_2O_2-OPD	0.046	8
Fluorescence (Turn-on)	Abtz-CdI_2-MOF	0.057	9
Fluorescence(Turn-off)	Graphene QDs	0.09	10
Fluorescence(Turn-on)	Calcein blue-Fe^{2+}	10	11
Fluorescence(Turn-on)	YCY_620	1.43	12
Fluorescence(Turn-off)	MoS_2 QDNS	0.0009	13
Fluorescence(Turn-off)	MoS_2 QDs	0.001	14
Fluorescence(Turn-off)	CQDs	200	15
Fluorescence(Turn-off)	QD@SiO_2	0.0125	16
Fluorescence(Turn-off)	β -CD@AuNCs	0.020	17
Fluorescence(Turn-off)	CDots-AuNCs	0.0029	18
Fluorescence(Turn-off)	GQDs	0.16	19
Fluorescence(Turn-off)	AgNPs	0.0001	20
Fluorescence (Turn-on)	UiO-67-DQ-PsO	0.00034	This work

References

1. Y. J. Diaz, Z. A. Page, A. S. Knight, N. J. Treat, J. R. Hemmer, C. J. Hawker and J. Read de Alaniz, *Chem. - Eur. J.*, 2017, **23**, 3562-3566.
2. W.-Q. Zhang, Q.-Y. Li, J.-Y. Cheng, K. Cheng, X. Yang, Y. Li, X. Zhao and X.-J. Wang, *ACS Appl. Mater. Interfaces*, 2017, **9**, 31352-31356.
3. L. Kong, Y. Zhang, H. Mao, X. Pan, Y. Tian, Z. Tian, X. Zeng, J. Shi, B. Tong and Y. Dong, *Faraday Discuss.*, 2017, **196**, 101-111.
4. S. E. Bustamante Fonseca, B. L. Rivas, J. M. Garcia Perez, S. Vallejos Calzada and F. Garcia, *J. Appl. Polym. Sci.*, 2018, **135**, n/a.
5. A. R. Longstreet, R. R. Chandler, T. Banerjee, L. Zane Miller, K. Hanson and D. Tyler McQuade, *Photochem Photobiol Sci*, 2017, **16**, 455-458.
6. H.-H. Tian, L.-T. Chen, R.-L. Zhang, J.-S. Zhao, C.-Y. Liu and N. S. Weng, *J. Solid State Chem.*, 2018, **258**, 674-681.
7. C. Zhao, Y. Liu and Y. Li, *Anal. Sci.*, 2015, **31**, 1035-1039.
8. C. Zhao, Z. Jiang, R. Mu and Y. Li, *Talanta*, 2016, **159**, 365-370.
9. Y. Cheng, J. Wu, C. Guo, X.-G. Li, B. Ding and Y. Li, *J. Mater. Chem. B*, 2017, **5**, 2524-2535.
10. J. Zhao, L. Zhao, C. Lan and S. Zhao, *Sens. Actuators, B*, 2016, **223**, 246-251.
11. D. Seto, T. Maki, N. Soh, K. Nakano, R. Ishimatsu and T. Imato, *Talanta*, 2012, **94**, 36-43.
12. Y.-K. Lin and Y.-C. Yeh, *Anal. Chem.*, 2017, **89**, 11178-11182.
13. N. Pallikkarathodi Mani, M. Ganiga and J. Cyriac, *Analyst*, 2018, **143**, 1691-1698.
14. X. Liu, W. Zhang, L. Huang, N. Hu, W. Liu, Y. Liu, S. Li, C. Yang, Y. Suo and J. Wang, *Microchim. Acta*, 2018, **185**, 1-8.
15. D. Bharathi, B. Siddlingeshwar, R. H. Krishna, V. Singh, N. Kottam, D. D. Divakar and A. AbdullahAlkheraif, *J. Fluoresc.*, 2018, **28**, 573-579.
16. B. Wang, M.-m. Chen, H.-q. Zhang, W. Wen, X.-h. Zhang and S.-f. Wang, *Microchim. Acta*, 2017, **184**, 3189-3196.
17. M. I. Halawa, F. Wu, T. H. Fereja, B. Lou and G. Xu, *Sens. Actuators, B*, 2018, **254**, 1017-1024.
18. Y.-S. He, C.-G. Pan, H.-X. Cao, M.-Z. Yue, L. Wang and G.-X. Liang, *Sens. Actuators, B*, 2018, **265**, 371-377.
19. H. Liu, N. Li, H. Zhang, F. Zhang and X. Su, *Talanta*, 2018, **189**, 190-195.
20. Q. Lu, X. Chen, D. Liu, C. Wu, M. Liu, H. Li, Y. Zhang and S. Yao, *Talanta*, 2018, **182**, 428-432.